polymer papers

Morphology and mechanical properties of a phase separated and a molecular composite 30% PBT/70% ABPBI triblock copolymer

Stephen J. Krause and Tim B. Haddock
Department of Chemical and Materials Engineering, Arizona State University, Tempe, AZ 85287, USA

and Gary E. Price
University of Dayton Research Institute, Dayton, OH 45469, USA

and W. Wade Adams
Polymer Branch, Materials Laboratory, Air Force Wright Aeronautical Laboratories, Wright-Patterson, OH 45433, USA
(Received 27 May 1987; accepted 28 July 1987)

The morphology of a triblock copolymer of 30% rigid-rod poly(*p*-phenylene benzobisthiazole) (PBT) and 70% semi-flexible coil poly(2,5(6)benzimidazole) (ABPBI) was examined by wide angle X-ray scattering and scanning and transmission electron microscopy. Samples that were vacuum cast from a solution formed a microphase separated film with 0.1 μm particles and platelets of well-oriented 10 nm PBT crystallites in a ductile ABPBI matrix. Fibres were dry-jet/wet-spun from an optically homogeneous solution into a water coagulation bath to inhibit large scale phase separation. Heat-treated fibre contained crystallites of PBT and ABPBI with lateral dimensions no larger than 3 nm, demonstrating that PBT molecular segments were well dispersed and that a rigid-rod, molecular level composite had been achieved. The molecular level dispersion and high orientation in the 'molecular composite' fibre resulted in excellent mechanical properties with a modulus of 100 GPa and a tensile strength of 1.7 GPa which were about an order of magnitude greater than for the vacuum cast copolymer film.

(Keywords: morphology; wide angle X-ray scattering; electron microscopy; poly(*p*-phenylene benzobisthiazole) (PBT); poly(2,5(6)benzimidazole) (ABPBI); copolymer; molecular composite)

INTRODUCTION

Currently, there is increasing interest in fabrication of rigid-rod molecular composites. A molecular composite is defined as a polymeric material consisting of two or more components which are dispersed at the molecular level at a scale no greater than a few nanometres. The purpose of forming a rigid-rod molecular composite is to reinforce a ductile matrix polymer with stiff, strong, rigid-rod polymer molecules. After synthesis, the key to producing a molecular composite is in controlling the morphology of the system in order to achieve the finest possible dispersion of the reinforcing rod molecules. Approaches to producing a molecular composite include special processing techniques and specific chemical synthesis methods. We report here the morphology of a new rigid-rod and flexible-coil triblock copolymer processed by different methods.

One method for producing a rigid-rod molecular composite is to create an intimate physical blend of rigid-rod molecules and flexible-coil molecules[1,2]. Takayanagi[3,4] studied several stiff-chain/flexible-coil polymer blends. He found that processing a blend of poly(*p*-phenylene terephthalamide) (PPTA) and nylon 6 or nylon 6/6 resulted in a dispersion of the reinforcing phase PPTA in the form of 30 nm diameter microfibrils throughout the matrix material. Hwang *et al.*[5] processed blends of rigid-rod poly(*p*-phenylene benzobisthiazole) (PBT) and semi-flexible coil poly-2,5(6) benzimidazole (ABPBI) into fibre and film. It was found that large scale phase separation was prevented when an optically homogeneous solution of 30% PBT/70% ABPBI was dry spun and then rapidly coagulated in water. In morphological studies of the 30% PBT/70% ABPBI heat-treated fibre and film by Krause and Adams[6] and Krause *et al.*[7], no phase separation was observed at a scale greater than 3 nm when samples were examined by wide angle X-ray scattering (WAXS) and scanning electron microscopy (s.e.m.) and transmission electron microscopy (t.e.m.). This demonstrated that a molecular composite had been achieved. A comparison of the moduli of oriented fibre of the PBT and ABPBI homopolymers to that of the physical blend also indicated that a molecular composite had been achieved according to the 'rule of mixtures' for a uniaxially reinforced composite[5]. The 'rule of mixtures' means that the modulus of the oriented blend fibre is proportional to the sum of the volume fractions of the individual components times their respective modulus in the oriented homopolymer fibre.

An alternative approach to physical blending of polymers for producing a molecular composite is to synthesize a block copolymer composed of flexible-coil segments and of rigid-rod block segments[8]. Ta-

0032-3861/88/020195-12$03.00

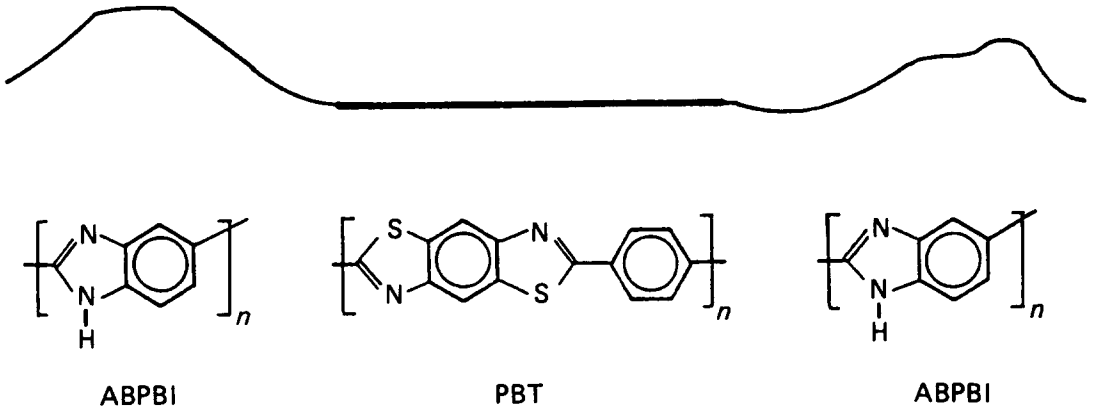

Figure 1 Chemical and molecular structure of a PBT/ABPBI triblock copolymer

kayanagi[3,4] studied a stiff-chain Aramid/flexible-coil nylon 6 copolymer and found that a 'fine dispersion' of the components was achieved, although the size of the dispersed phase was not quantified. Tsai *et al.*[8] have recently reported on the synthesis and properties of a triblock copolymer of PBT and ABPBI. The chemical and molecular structure of the copolymer is shown in *Figure 1*. A comparison of the moduli of oriented fibres of the homopolymers to that of the copolymer indicated that a molecular composite had been achieved according to the 'rule of mixtures'[5]. However, a detailed morphological study directly examining the level of dispersion of the components in this material has not yet been carried out.

The goal of this study was to characterize with WAXS, s.e.m. and t.e.m. the structure and morphology of the PBT/ABPBI triblock copolymer synthesized by Tsai *et al.*[8] Additionally, structural and morphological results of this study on fibre and film of the PBT/ABPBI block copolymer were compared with the earlier results of a PBT/ABPBI physical blend[6,7].

BACKGROUND

PBT fibre

PBT is a rigid-rod, extended chain, aromatic heterocyclic polymer with high strength, high modulus, and excellent environmental and thermal resistance. PBT has only on-axis bond rotations, resulting in extended rigid-rod molecules. Its chemical structure is shown in *Figure 1*. The unit cell structure was studied by Adams *et al.*[9], Roche *et al.*[10] and Odell *et al.*[11] The non-primitive unit cell is monoclinic with the axis lengths of $a = 1.196$ nm, $b = 0.355$ nm and $c = 1.235$ nm, and a unit cell angle of $\gamma = 100.9°$ (ref. 10). The PBT molecular axis is parallel to the c axis and molecules are located in the corners and centre of the a–b plane of the unit cell. For an individual PBT molecule, the plane of the benzobisthiazole ring structure is $-5°$ from the a axis and the phenylene plane is 25° from the a axis.

The morphology and properties of PBT fibre have been extensively studied[12–15]. Results from WAXS[15] and t.e.m.[12,13] have shown that spun, drawn and heat-treated PBT fibre has very high molecular and crystallite orientation. High molecular orientation and chain perfection were demonstrated from t.e.m. selected area electron diffraction (s.a.e.d.) results in which 27 orders of meridional reflections were observed[12]. High crystallite orientation was demonstrated from WAXS results in which a c-axis Hermann's orientation factor of 0.99 was observed[14]. PBT molecules were generally found to be two-dimensionally (2-D) ordered laterally and were axially disordered along the fibre axis[12], although limited 3-D ordering was occasionally observed[13] in t.e.m. lattice fringe images. The heat-treated PBT fibre contained crystallites with dimensions of about 20 nm along the c-axis, 9 nm along the a-axis and 6 nm along the b-axis[7,12]. The high molecular and crystallite orientation along the fibre axis contributes to very high axial mechanical properties[12,14]. S.e.m.images of a PBT fracture surface showed that the fibre has little ductility, in agreement with stress–strain curves which show linear elastic behaviour to the fracture point[16]. Allen *et al.*[15] studied the effect of heat treatment on as-spun PBT fibre and reported moduli up to 320 GPa and tensile strengths up to 3.1 GPa for the heat-treated fibre. The results of mechanical property studies on PBT, ABPBI, a 30% BPT/70% ABPBI physical blend, and a 30% PBT/70% ABPBI triblock copolymer are summarized in *Table 1*.

Table 1 Mechanical testing results for PBT, ABPBI and 30% PBT/70% ABPBI fibres and films

Sample	Modulus GPa, (Mpsi)	Tensile strength, MPa (ksi)	Elongation to break (%)
PBT fibre	320 (48)	3100 (460)	1.1
ABPBI fibre	36 (5.3)	1100 (160)	5.2
30% PBT/70% ABPBI $C > C_{cr}$ blend film	1.1 (0.16)	35 (5.1)	5.6
30% PBT/70% ABPBI $C < C_{cr}$ blend fibre	120 (17)	1300 (180)	1.4
30% PBT/70% ABPBI $C > C_{cr}$ copolymer film	2.4 (0.35)	220 (32)	43
30% PBT/70% ABPBI $C < C_{cr}$ copolymer fibre	100 (15)	1700 (250)	2.4

ABPBI fibre

ABPBI is an aromatic heterocyclic semi-flexible coil polymer with excellent thermal and mechanical properties[17]. Its chemical structure is shown in *Figure 1*. ABPBI can assume a coil-like structure due to off-axis rotations about its backbone bonds. It has not been

studied as extensively as PBT and the unit cell of ABPBI has not been reported. However, the unit cells of polymers poly-2,6-benzothiazole (ABPBT) and poly-2,5-benzoxazole (ABPBO) have been reported to be orthogonal (pseudo-orthorhombic) by Fratini *et al.*[18] On the basis of the similarity of the chemical structure of ABPBI to that of ABPBT and ABPBO, a preliminary crystal structure has been proposed for ABPBI with an orthorhombic unit cell with axis lengths $a=0.72$ nm, $b=0.35$ nm and $c=1.17$ nm[7].

The morphology of ABPBI has received limited study. It was found that stretching of ABPBI film caused negligible changes in d-spacings but produced higher orientation[7]. When as-spun fibres of ABPBI were heat treated, the length of the *a* axis was reduced from 0.83 to 0.72 nm due to improved lateral packing of chains. Krause *et al.*[7] found that the heat-treated fibre contained crystallites which had lateral dimensions no larger than 3 nm. Crystallites were three-dimensionally ordered within the fibre, but only two-dimensionally ordered at the fibre surface. Crystallites and molecules were moderately well-oriented with respect to the fibre axis. The molecular orientation was demonstrated from t.e.m. s.a.e.d. results in which three orders of meridional reflections were observed. The crystallite orientation was demonstrated from WAXS results in which a *c*-axis orientation factor of 0.91 was observed. S.e.m. images of an ABPBI fibre fracture surface showed the presence of drawing and micronecking which is in agreement with mechanical testing results which showed that ABPBI fibre had higher ductility (5.2%) and lower strength (1100 MPa) when compared to PBT (1.1% and 3100 MPa, respectively)[7]. This is due in part to the flexible-coil chain architecture of ABPBI and also the lower molecular and crystalline orientation in ABPBI fibre compared with PBT fibre. The mechanical properties of ABPBI have been studied by Hwang *et al.*[5] who reported a modulus of 36 GPa and a tensile strength of 1100 MPa for heat-treated fibre.

Polymer phase compatibility

Phase separation of the components of a polymer blend or a block copolymer can significantly affect mechanical properties. In macroscopic composite theory the effect of the geometry of the reinforcing phase can be evaluated in terms of a parameter known as the *aspect ratio*, defined as $2L/D$, where L is the length and D is the diameter of the reinforcing phase. High aspect ratios (preferably greater than 100) provide efficient reinforcement of matrix material by the reinforcing phase[19].

It has been proposed that the effect of reinforcement of a ductile polymer matrix by rigid-rod molecules or rigid-rod molecular segments (of a copolymer) is analogous to the reinforcing effect of high aspect-ratio fibre on the properties of macroscopic composites[1,5]. If we consider, for example, that rigid-rod PBT molecules or molecular segments can be dispersed singularly or in small bundles (<3 nm) in an ABPBI matrix, the aspect ratio of a PBT molecule or segment may be as high as 330, if the length and diameter are about 100 and 0.6 nm, respectively. Even for bundles of PBT molecules or segments 2–3 nm wide, an aspect ratio of 70–100 would be maintained and provide efficient reinforcement.

If, alternatively, rigid-rod molecules phase separate or molecular segments microphase separate on a large scale from the flexible-coil matrix polymer, then the aspect ratio of the rigid-rod reinforcing phase would be reduced to a low value. A low aspect ratio and reduced amount of reinforcing component in the matrix would not be expected to provide efficient reinforcement.

Hwang *et al.*[5,20] investigated solution properties, processing and mechanical properties of PBT/ABPBI physical blends in a solvent of methane sulphonic acid (MSA) and interpreted their results in terms of Flory's theory of phase equilibria of rigid-rod and flexible-coil polymer systems[21,22]. It was found from optical microscopy that when the total concentration (C) of the polymer in the solvent was above a critical concentration (C_{cr}), liquid crystalline domains formed in an optically isotropic liquid, demonstrating that the solution had phase separated. The C_{cr} for phase separation varied from 2 to 6% polymer in solution as the ratio of PBT to ABPBI decreased. C_{cr} decreased when temperature decreased and when the molecular weight of PBT increased, in accordance with Flory's theory[22]. In another study of phase equilibria of a block copolymer, Tsai *et al.*[8] found that the critical concentration was 5.8% for phase separation of rigid-rod segments from a 30% PBT/70% ABPBI triblock copolymer in MSA compared with 3% for phase separation of rigid-rod molecules from a 30% PBT/70%ABPBI physical blend in MSA. This shows that phase separation was inhibited by combining PBT and ABPBI in the form of a copolymer rather than in the form of a physical blend.

Physical blend cast film

The effect of phase separation on the morphology of a physical blend of 30% PBT/70% ABPBI has been studied by Hwang *et al.*[5] and Krause *et al.*[7]. S.e.m. images of PBT/ABPBI vacuum cast films showed brittle, 0.1–4 μm long, ellipsoidal particles separated from the adjacent ductile matrix material. The removal of solvent during the casting process caused the polymer concentration to rise above C_{cr} and induce thermodynamically favoured phase separation in the binary rod/coil blend[22]. The liquid crystal phase separation was manifested in the solid state by the formation of elongated second-phase particles 0.1–4 μm in length. S.e.m. backscattering studies of the films showed that the ellipsoidal particles were composed chiefly of sulphur-rich PBT. The ellipsoidal particle shape was expected since the geometry of the rod-like PBT molecules would cause them to align side by side in elongated liquid crystalline domains during phase separation. This was confirmed by Krause and Adams[6] who reported that the particles were chiefly composed of aggregates of 10 nm PBT crystallites moderately well aligned with the longitudinal axis of the ellipsoids. The matrix material was ductile and composed chiefly of ABPBI. *Figure 2a* shows a schematic representation of the phase-separated PBT-rich particles in the ABPBI-rich matrix. As listed in *Table 1*, the modulus is 1.1 GPa and tensile strength is 35 MPa. These values are roughly one order of magnitude less than ABPBI fibre and two orders of magnitude less than PBT fibre. These very low properties, compared with the homopolymer fibre, are due to phase separation, random orientation and poor adhesion of the PBT-rich particles to the ABPBI-rich matrix.

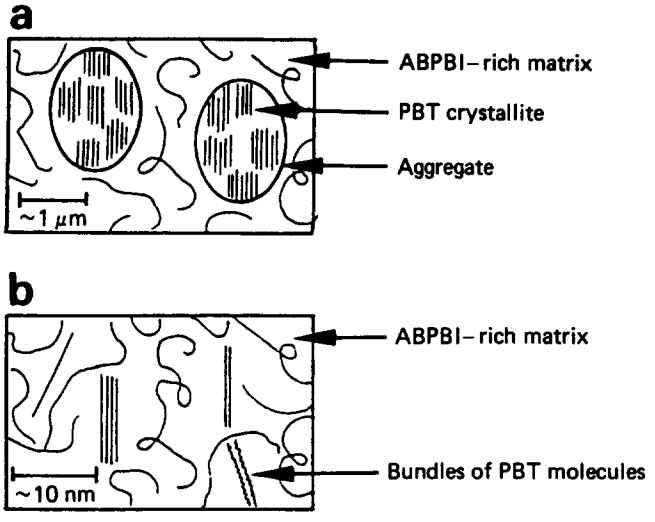

Figure 2 Models for morphology of a 30% PBT/70% ABPBI physical blend (a) vacuum cast film from $C > C_{cr}$ solution and (b) spun fibre from $C < C_{cr}$ solution

Physical blend spun fibre

The effect on properties and morphology of processing a 30% PBT/70% ABPBI physical blend by dry-jet/wet spinning has been studied by Hwang *et al.*[5] and Krause *et al.*[7] S.e.m. images of a fibre fracture surface showed reduced fibrillation (compared with PBT fibre) and no phase separation to the 20 nm resolution limit of the instrument. WAXS and t.e.m. showed that heat-treated fibre contained well oriented molecules and crystallites of both ABPBI and PBT which were less than 3 nm in width. The ABPBI molecules and crystallites were more oriented in the blend fibre than in the pure ABPBI fibre due to enhanced orientation of ABPBI molecules by entanglement with PBT molecules. PBT molecules and crystallites were less oriented in the blend fibre than in pure PBT fibre due to the ABPBI molecules that inhibited orientation. Crystallites of PBT and ABPBI were less than 3 nm in size as a result of immobilization of the entangled and dispersed PBT and ABPBI molecules during rapid coagulation of the homogeneous solution in the fibre spinning process. Individual molecules or crystallites of PBT smaller than 3 nm in lateral size may have been present in the fibre, but their presence could not be determined from t.e.m. Since the aspect ratio of the reinforcing phase of PBT molecules or molecular bundles was very high it was stated that a molecular composite had been achieved. *Figure 2b* shows a model of the morphology of the physical blend molecular composite. Good dispersion, excellent adhesion and high orientation of PBT in ABPBI gave efficient reinforcement which resulted in high values of mechanical properties in the molecular composite fibre, especially when compared with the phase-separated film. Properties are listed in *Table 1*.

In the physical blend system the 'molecular composite' fibre ($C < C_{cr}$) had values of strength and modulus which were roughly one order of magnitude greater than the physical blend phase-separated fibre (values appear in ref. 7) and two orders of magnitude greater than the phase-separated ($C > C_{cr}$) film. The modulus of the 'molecular composite' fibre is about one-third of that of pure PBT fibre which corresponds reasonably well to the 'rule of mixtures' for a uniaxially reinforced composite. However, the use of the 'rule of mixtures' has been based upon the measured, not the theoretical, modulus of PBT which raises questions as to the applicability of the 'rule of mixtures' for molecular composites. This question will be considered further in the discussion of results in this study. The tensile strength is only slightly more than that of the ABPBI fibre, but tensile strength is strongly dependent on flaws and processing variations which may have limited possible improvements.

The value of elongation to break for the 'molecular composite' fibre is reduced to about one-quarter of that for the phase-separated film. This occurs both because phase separation of PBT gives a larger volume fraction of ductile ABPBI in the matrix and because high orientation of molecules in the 'molecular composite' fibre limits elongation prior to fracture.

Copolymer film and fibre

Also included in *Table 1* are the mechanical property results of the 30% PBT/70% ABPBI block copolymer from Tsai *et al.*[8] Mechanical properties of copolymer fibre spun from homogeneous solution ($C < C_{cr}$) are similar to those of physical blend ($C < C_{cr}$) fibre, which makes it likely that a molecular composite fibre has formed. The slightly higher (30%) strength of the copolymer fibre may be due to processing differences or structure and morphology differences. Modulus and strength of the copolymer fibre are roughly one order of magnitude larger than the copolymer film vacuum cast from a concentrated solution ($C > C_{cr}$). The elongation to break is much greater for the copolymer film than the fibre. The significance of this and other mechanical property results will be discussed and correlated to morphological results later in this report.

EXPERIMENTAL RESULTS

Materials processing

The synthesis of PBT/ABPBI triblock copolymers has been described by Tsai *et al.*[8] ABPBI monomer was reacted from the ends of PBT molecules to form triblock copolymer molecules such that the molar ratio of the two components along a given molecule was 35% ABPBI/30% PBT/35% ABPBI. This was referred to as a 30% PBT/70% ABPBI block copolymer. The molecular weight for the original PBT block component was estimated by intrinsic viscosity measurements to be 41 kg mol^{-1}. The length of the PBT segment and of each of the ABPBI segments is about 100 nm.

The techniques for processing the copolymer into fibre and film were reported previously by Hwang *et al.*[5] A mixture of 97.5 vol% MSA and 2.5 vol% chlorosulphonic acid (CSA) was the solvent for the polymers. The critical concentration of the copolymer in the solvent was 5.8 wt%.

Fibre was spun by extruding $C < C_{cr}$ solution through a spinneret die into a water coagulating bath. The fibre was dry-jet/wet-spun to a high draw ratio in the air gap between the die and the water bath. The wet fibre was neutralized in NH_4OH overnight, rinsed in distilled water, and heat treated under tension at elevated temperatures in air.

The processing of vacuum cast film has been described by Husman *et al.*[2] Solvent from a $C < C_{cr}$ solution was removed in a sublimator, with the slowly decreasing

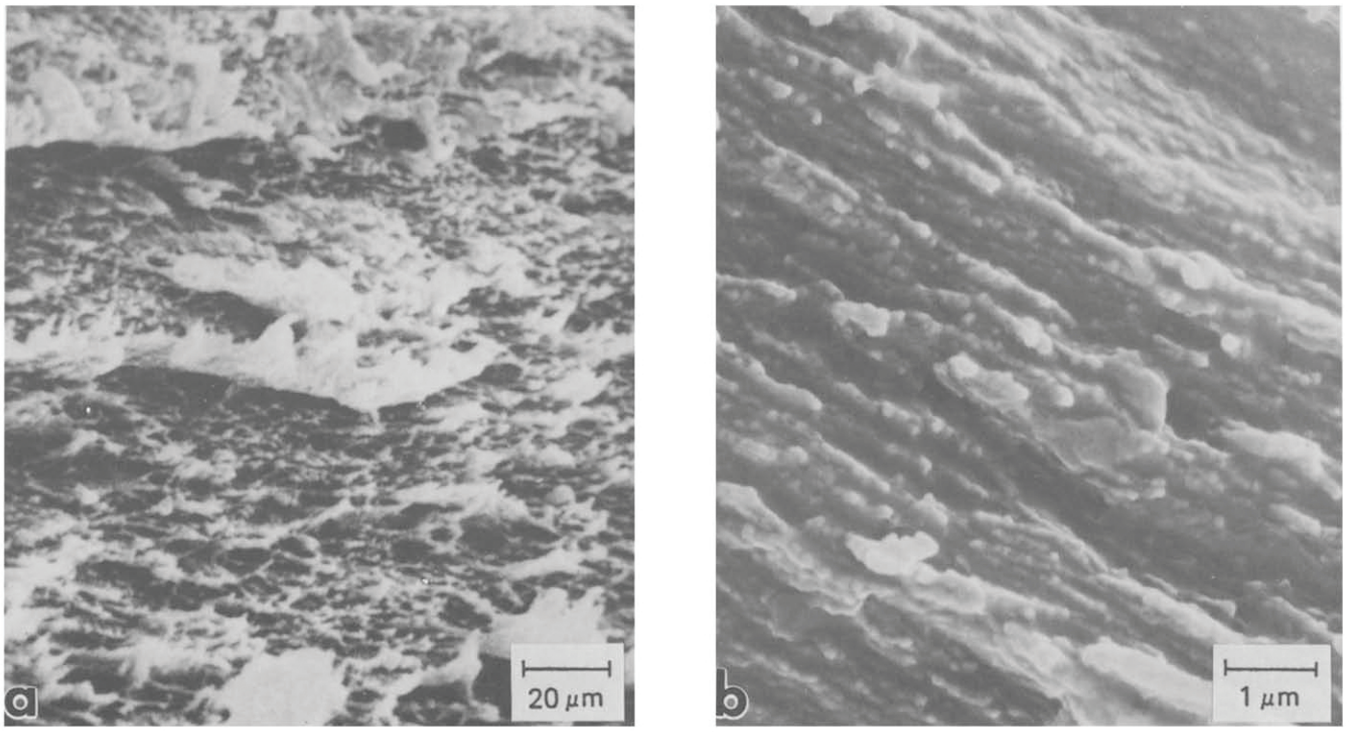

Figure 3 S.e.m. images of 30% PBT/70% ABPBI vacuum cast copolymer film at (a) lower and (b) higher magnification

amount of solvent resulting in a concentrated ($C \gg C_{cr}$) solution and, ultimately, a cast film. The film was neutralized, rinsed and dried in a vacuum oven to remove residual solvent.

Scanning electron microscopy (s.e.m.)

Samples were prepared for s.e.m. imaging by submerging fibre and film in liquid nitrogen and then fracturing. The fracture surfaces were sputter-coated with gold-palladium to prevent charging during imaging and were examined on an ISI Alpha 9 s.e.m. at 10 kV at magnifications from × 100 to × 10000. Images were recorded on Polaroid P/N 55 film.

Wide angle X-ray scattering

The fibre sample was prepared for WAXS by winding approximately 10 cm of a single filament around a cardboard holder. The film sample for WAXS required no special preparation techniques. The WAXS photographs were recorded with flat-film Statton (Warhus) cameras. CuKα radiation was generated by an Elliot GX20 rotating anode X-ray generator with a nickel filter. The sample-to-film distances were 29.2 ± 0.2 mm for the two Statton cameras, calibrated by the known crystalline reflections of a standard silicon powder, SRM 640.

Transmission electron microscopy (t.e.m.)

T.e.m. samples were prepared by ion thinning since copolymer film and fibre were not amenable to preparation by more traditional detachment replication techniques[12]. In ion-thinned samples damage occurred at the thinnest edges of some sample areas due to the bombardment of the copolymer with argon ions. Many undamaged areas were, however, available for examination. T.e.m. images and s.a.e.d. patterns were taken on Kodak SO-163 film on a JEOL 100CX at an accelerating voltage of 100 kV using low dose techniques.

RESULTS AND DISCUSSION

Scanning electron microscopy (s.e.m.)

Cast copolymer film. The fracture surface of the 30% PBT/70% ABPBI $C > C_{cr}$ vacuum cast copolymer film is shown in *Figure 3a* at lower magnification, and in *Figure 3b* at higher magnification. The fracture surface at low magnification is flat and rather 'spotty'. At higher magnification the 'spots' are actually seen to be a combination of particles, rows of particles and some small platelets embedded with the matrix material. There is a great deal of fine scale micronecking on the larger, rather flat surfaces. Frequently, micronecks are terminated by a small particle or a small line of particles.

In previous studies[5,7] on phase-separated film and fibre of a 30% PBT/70% ABPBI physical blend, s.e.m. images showed 0.1–4 μm particles separated from the matrix which resemble the particles observed here. However, the particles in the block copolymer show much better adhesion to the matrix than the particles in the cast film of the physical blend. In the copolymer this is due to the chemical bond between the PBT molecular segments in the particles and ABPBI molecular segments in the matrix whereas in the physical blend there is evidently only a mechanical bond between the PBT in the particles and the ABPBI in the matrix. In the physical blend such particles were identified as phase-separated material composed chiefly of PBT crystallites. In the block copolymer, t.e.m. results presented later also show that the small particles are composed chiefly of microphase separated PBT crystallites. This is reasonable since the PBT molecular block segments are about 0.1 μm long. Although phase-separated particles in the physical blend film grew to as large as 4 μm long ellipsoids, it is highly unlikely that the particles in the copolymer film could grow much larger in length than 0.1 μm since the end of each 0.1 μm PBT segment is terminated with a flexible-

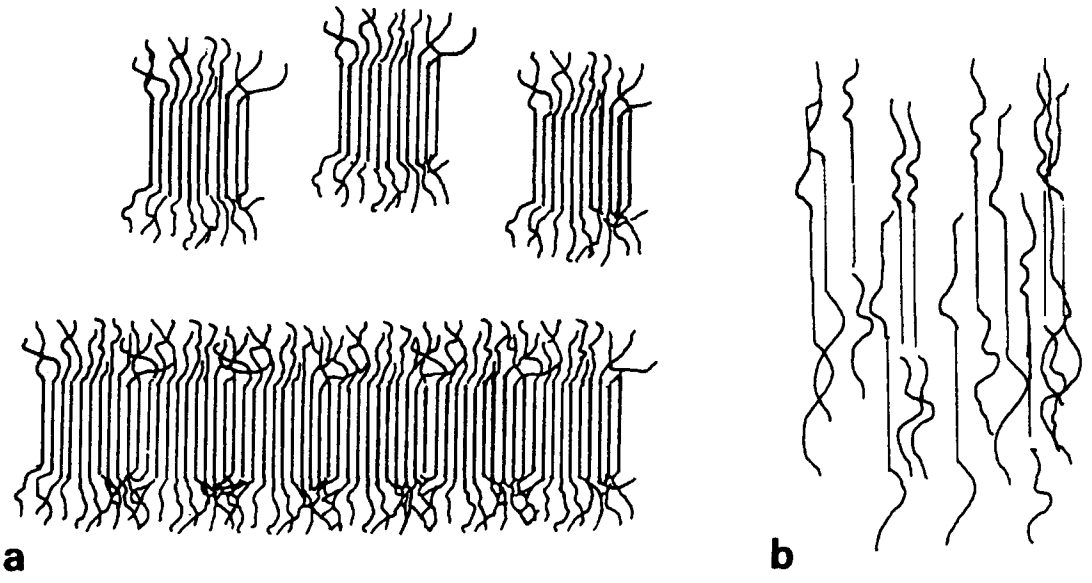

Figure 4 Models for morphology of a 30% PBT/70% ABPBI copolymer (a) vacuum cast film from $C > C_{cr}$ solution and (b) spun fibre from $C < C_{cr}$ solution

coil ABPBI segment. It might, however, be possible for the rigid-rod PBT molecular segments to phase separate and coalesce with lateral growth between adjacent rod segments. There are indications that this occurred since either small platelets or strings of four to five microphase-separated particles up to 0.4 μm in width are occasionally observed. A model for the morphology of phase-separated material in the cast copolymer film is shown in *Figure 4a*.

In the previous study on the phase-separated physical blend film it was also shown that the matrix material was composed chiefly of ABPBI[7]. It is likely that the matrix in the microphase-separated copolymer film is also chiefly ABPBI. This is indicated by the ductile fracture behaviour, which is characteristic of ABPBI, of the matrix adjacent to the microphase separated particles and platelets. Large scale 0.5–1 μm necking, which was observed for the phase-separated physical blend film, is unlikely to occur with the copolymer film since the flexible-coil segments of the triblock copolymer molecules only extend a maximum of about 0.1 μm from each end of the PBT segment. In the microphase-separated form it is thus unlikely that ABPBI in the block copolymer extends continuously beyond 0.1–0.3 μm. This accounts for the small scale micronecking observed here.

Spun copolymer fibre. The fracture surface of the 30% PBT/70% ABPBI $C < C_{cr}$ spun fibre is shown in *Figure 5a* and *b* at low magnification, and in *Figure 5c* at higher magnification. The low magnification images show that the fibre has split through the middle parallel to the fibre axis. This indicates that there is at least moderate orientation of the molecules along the fibre axis. Data presented later in this study indicate that the molecules and crystallites are well oriented along the fibre axis. The fracture surface itself is rather flat and approximately perpendicular to the fibre axis. It is somewhat unusual that there is high molecular orientation and yet a flat fracture surface across the fibre with little or no longitudinal fibrillation. This indicates that although there is high axial strength along the fibre, there is also moderate lateral strength across the cross-section of the fibre which would inhibit fibrillation. The structure of the fracture surface contrasts sharply with the structure observed in other types of high-strength, high-modulus fibres. PBT fibre fibrillates extensively upon fracture, as expected, due to its high axial strength and low lateral strength[12]. The 30% PBT/70% ABPBI physical blend fibre, which has relatively high strength, fibrillates moderately upon fracture, but to a more limited extent than PBT, due to its moderate ductility and lateral strength. On the other hand, ABPBI fibre, whose strength and modulus are about an order of magnitude lower than that of PBT, fibrillates little upon fracture, as expected, both due to reduced orientation and moderately high ductility and lateral strength. Thus, it appears that the lack of fibrillation in the 30% PBT/70% ABPBI copolymer fibre is an indication that, if the orientation is similar to that of the 30% PBT/70% ABPBI physical blend fibre, it has greater ductility and higher lateral strength than the physical blend fibre.

The higher magnification image of the copolymer film in *Figure 5c* shows unusual and significantly different morphological features in the skin region near the fibre surface compared with the core region near the centre of the fibre. The skin region is composed of solid material while the interior region has elongated voids running along the fibre axis. It is likely that the voids are a result of the fibre spinning process. The diameter of the fibre of 60–70 μm is larger than that currently used, and may have induced void formation during spinning. It may also be that residual solvent in the core left voids behind after being removed. It is important to note here that since the voids occupy about 35% of the cross-sectional area, it is likely that the mechanical properties of the fibre would be more than 50% higher than those measured, if the fibre had been free of voids.

Morphology and property differences between the fibre surface and the fibre interior are frequently referred to as a skin-core effect. A skin-core effect exists for many ordered polymer fibre systems, including PPTA[23,24], PBT[12] and ABPBI[7]. The role of the skin-core structure in mechanical behaviour of fibre is not at all well understood, but it may have a significant effect on properties, especially in composite applications.

Figure 5b shows that, along the length of the skin, there

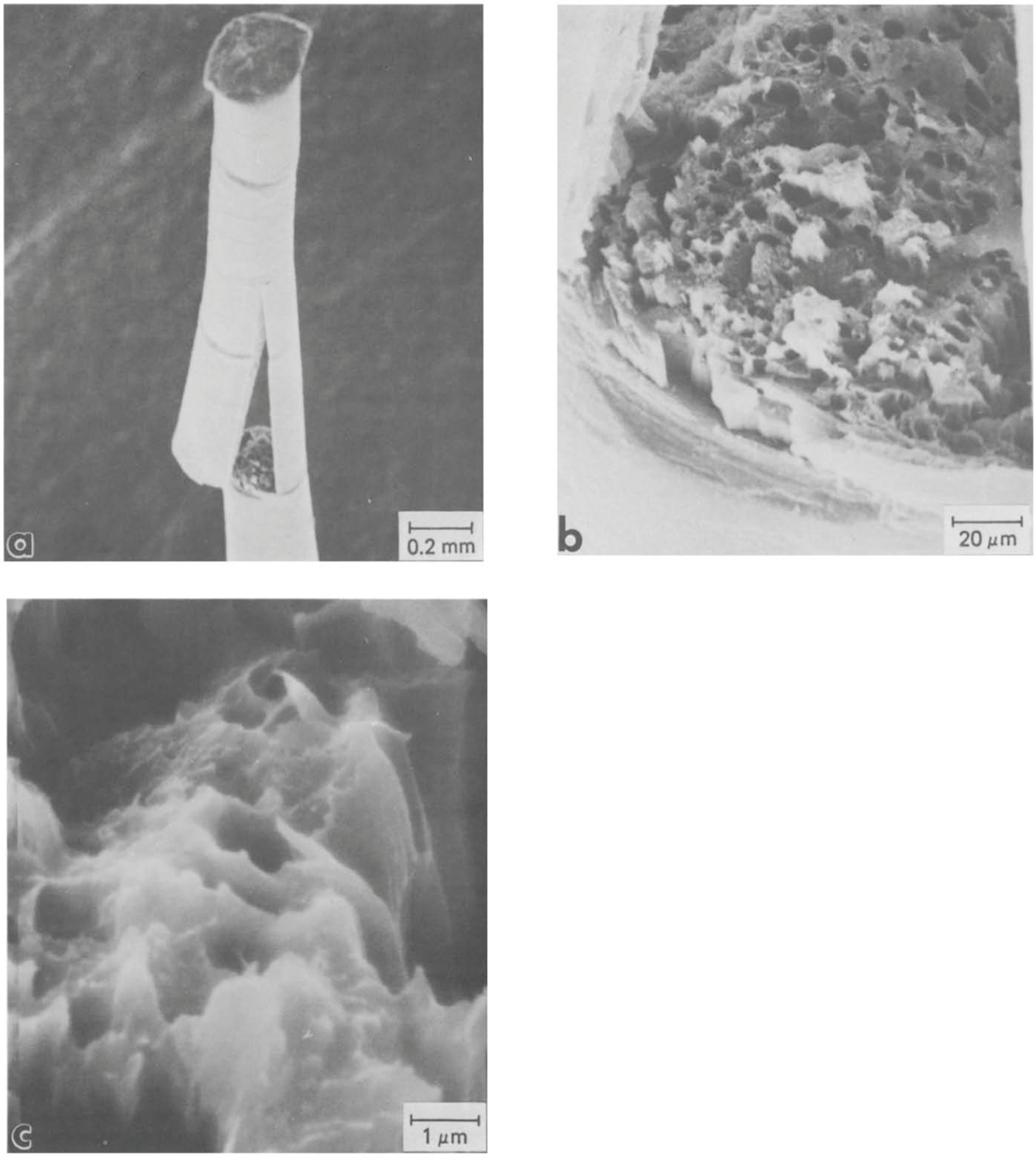

Figure 5 S.e.m. images of 30% PBT/70% ABPBI spun copolymer fibre at (a) very low, (b) low and (c) higher magnification

are longitudinally aligned layers with sharp boundaries which are interconnected in a region between the surface and about 5–10 μm into the interior. There are steps at the boundaries of these layers which range in height from about 0.1 to greater than 5 μm. The fracture surface on top of some of these layers is flat or stepped while on other surface areas it shows considerable micronecking. Upon closer inspection it is seen that even the flattest surface areas exhibit some extremely fine micronecking. The presence of the limited to moderate micronecking indicates that the fibre has moderate ductility.

The fibre interior contains elongated voids which are 1–5 μm long and decrease in size from about 1 to 3 μm at the centre of the fibre to about 0.2–0.5 μm in diameter towards the skin. As with the morphology of the fracture surface in the skin region, the fracture surface in the interior region is generally flat, but upon closer inspection many regions appear to have a significant amount of shallow micronecking. The step structure is also present here with steps ranging in size from a fraction of a micron to 2 to 3 μm. The origin of the step structure is unclear.

The fibre, unlike the vacuum cast film does not appear to contain any phase-separated particles to the 20 nm resolution limit of the s.e.m. However, it may be difficult

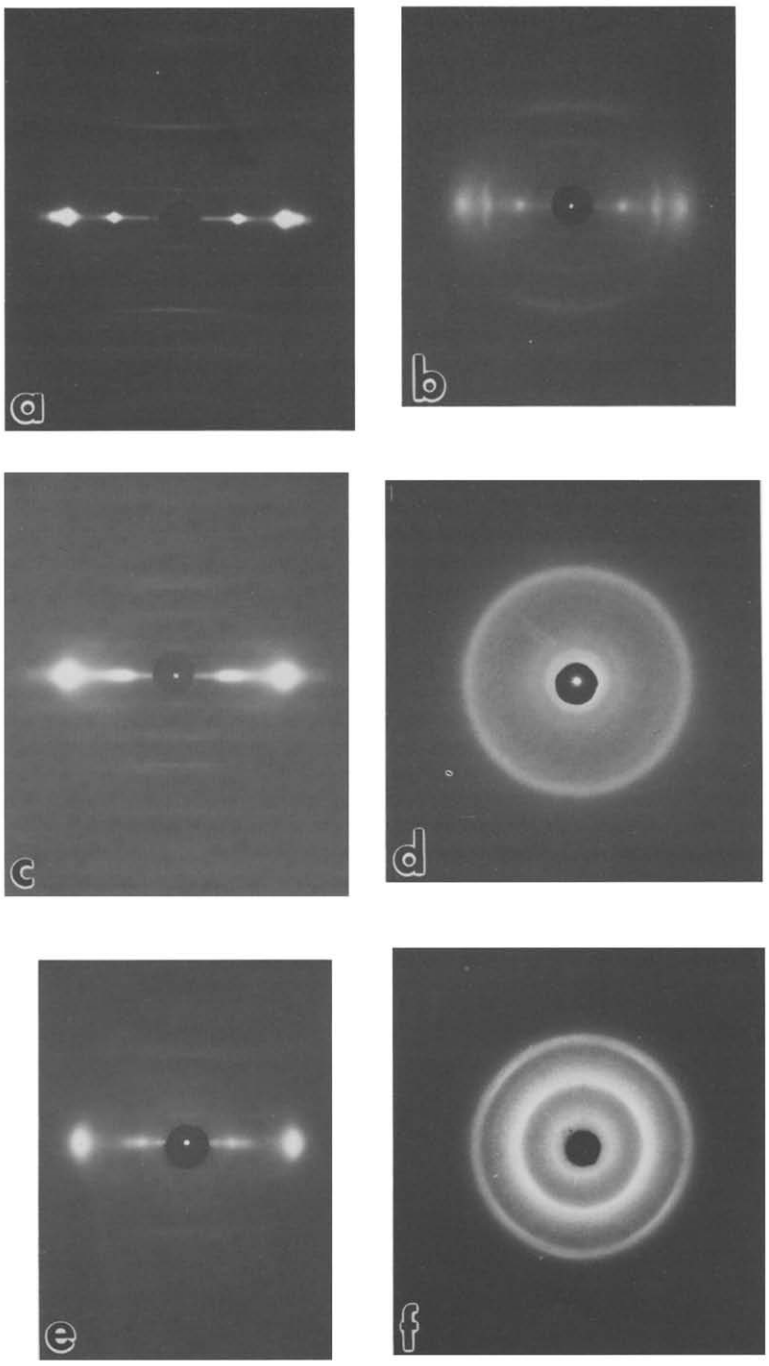

Figure 6 WAXS Laue photographs of (a) PBT fibre, (b) ABPBI fibre, (c) 30% PBT/70% ABPBI physical blend spun fibre, (d) 30% PBT/70% ABPBI physical blend vacuum cast film, (e) 30% PBT/70% ABPBI copolymer spun fibre, (f) 30% PBT/70% ABPBI copolymer vacuum cast film

to distinguish between very fine particles on the surface and very fine micronecking. It is reasonable to place an initial upper size limit of 20 nm, as determined by s.e.m., on any possible phase separation in the copolymer fibre which has been processed from homogeneous solution. A similar conclusion was reached for s.e.m. studies of 30% PBT/70% ABPBI physical blend fibre spun from a homogeneous solution[5,7]. The question of phase separation will receive additional consideration in the section on t.e.m. studies.

Wide angle X-ray scattering

To compare the structure of samples in this study with that of samples from a previous study[7], the WAXS photographs have been included in *Figure 6* for (a) PBT fibre, (b) ABPBI fibre, (c) spun fibre and (d) cast film of a 30% PBT/70% ABPBI physical blend. The d-spacings in *Table 2* were determined from the reflections in the photographs.

Cast copolymer film. The WAXS pattern for 30% PBT/70% ABPBI $C > C_{cr}$ vacuum cast film is shown in *Figure 6f.* There are four uniform Debye rings present. The 0.58 nm reflection, which corresponds to an equatorial spacing in PBT fibres, indicates PBT crystallites are present. The 0.35 nm reflection can be a combined reflection for both PBT and ABPBI, although it is only certain that PBT crystallites are present from the

Table 2 The WAXS d-spacings (nm) for PBT, ABPBI and 30% PBT/70% ABPBI fibres and films[a]

			30% PBT/70% ABPBI			
			Physical blend		Copolymer	
	PBT fibre	ABPBI fibre	$C > C_{cr}$ film	$C < C_{cr}$ fibre	$C > C_{cr}$ film	$C < C_{cr}$ fibre
Equatorial (h k 0)	–	–	–	–	–	1.28
d-spacings	–	0.72	0.83	0.74	–	0.80
	0.58	–	0.60	0.61	0.58	0.63
	–	0.45	–	–	–	–
	0.35	0.35	0.35	0.35	0.36	0.36
	0.32	–	–	–	–	–
	0.30	–	–	–	0.28	–
Off-axis (h k l)	–	0.51	–	–	–	–
d-spacings	–	0.43	–	–	–	–
	–	0.32	–	–	–	–
Meridional (0 0 l)	1.25	–	–	1.27	1.25	1.27
d-spacings	–	(1.17)	–	–	–	–
	0.63	–	–	0.60	–	0.60
	–	0.58	–	–	–	–
	0.42	–	0.42	0.42	0.42	0.42
	–	0.39	–	0.39	–	0.39
	0.31	–	–	0.31	–	0.31
	–	0.29	–	–	–	0.29
	0.24	–	0.25	0.25	–	–
	–	(0.23)	–	0.23	–	–

[a] Values in parentheses are calculated, not measured

0.58 nm reflection. Additionally, there are 1.25 and 0.42 nm reflections which correspond to meridional spacings in pure PBT fibres. The slightly arced rings indicate there is slight overall orientation of crystallites in the film. The equatorial reflections from crystallites in the film are moderately sharp, which indicates crystallites are of an intermediate size. There are no reflections present which are characteristic of ABPBI crystallites. The results are similar to those observed for the WAXS of the vacuum cast film of the 30% PBT/70% ABPBI physical blend shown in *Figure 6d*.

Spun copolymer fibre. The WAXS pattern for 30% PBT/70% ABPBI $C < C_{cr}$ fibre shown in *Figure 6e* shows highly-arced equatorial reflections, indicating well-oriented crystallites and flat meridional reflections, sometimes in pairs, extending out to high orders, indicating well-oriented molecules of both species. This copolymer fibre has equatorial and meridional spacings present which correspond to those in both PBT and ABPBI fibres. The 0.80 nm equatorial reflection, a characteristic ABPBI equatorial reflection in heat-treated fibre, indicates ABPBI crystallites are present. Additionally, there are at least two meridional reflections present (at 0.39 and 0.29 nm) which are characteristic ABPBI meridional spacings. This indicates that molecules of ABPBI are well ordered and moderately oriented in the blend fibre. In fact, the meridional reflections characteristic of ABPBI in the blend fibre are flatter and sharper than those in pure ABPBI fibre. The physical blend fibre also displayed similar WAXS features. Hwang *et al.*[5] have attributed higher orientation of the ABPBI molecules in a physical blend spun fibre to entanglement of ABPBI with PBT which extends ABPBI molecules along the well oriented PBT molecules resulting in higher orientation of the ABPBI molecules. The higher orientation of the ABPBI molecules in the block copolymer than in pure ABPBI fibre is also probably due to entanglement and extension of ABPBI with PBT which results in higher orientation of the ABPBI molecules. Although the alignment of ABPBI molecules and crystallites increases in the copolymer fibre, the diffuseness of the characteristic 0.74 and 0.44 nm reflections indicates that crystallite size remains relatively small.

The 0.63 nm spacing, a characteristic PBT equatorial reflection, indicates PBT crystallites are present. Additionally, there are four meridional reflections (1.27, 0.604, 0.420 and 0.31 nm) which are characteristic PBT meridional reflections. This indicates that the molecules of PBT are well-oriented in the copolymer fibre. However, as with the blend fibre, there are not as many orders of meridional reflections, nor are the characteristic PBT meridional reflections as flat or as sharp as those in the pure PBT fibre which indicates that PBT molecules are less oriented than in pure PBT fibre. This is probably due to the presence of semi-flexible coil ABPBI molecular segments which inhibit orientation of rigid-rod PBT molecules during the spinning of copolymer fibre. Also, the solution is not spun from a nematic liquid crystal state as it is in spinning of pure PBT fibre.

A major difference between the PBT in the copolymer fibre and the pure PBT fibre is the relative diffuseness of the characteristic 0.58 nm PBT reflection and the composite 0.35 nm reflection. The diffuseness of these reflections indicates that the crystallite size for PBT is much smaller in the copolymer fibre than in the pure PBT fibre. This small crystallite size is a result of the processing conditions in which there is no large-scale phase separation in the $C < C_{cr}$ solution prior to fibre spinning. After spinning and during coagulation large-scale phase separation of PBT from ABPBI is inhibited by the entanglement of ABPBI molecules which also inhibits growth of larger or more ordered PBT crystallites.

There is another interesting trend present in the data. One of the characteristic PBT equatorial reflections and

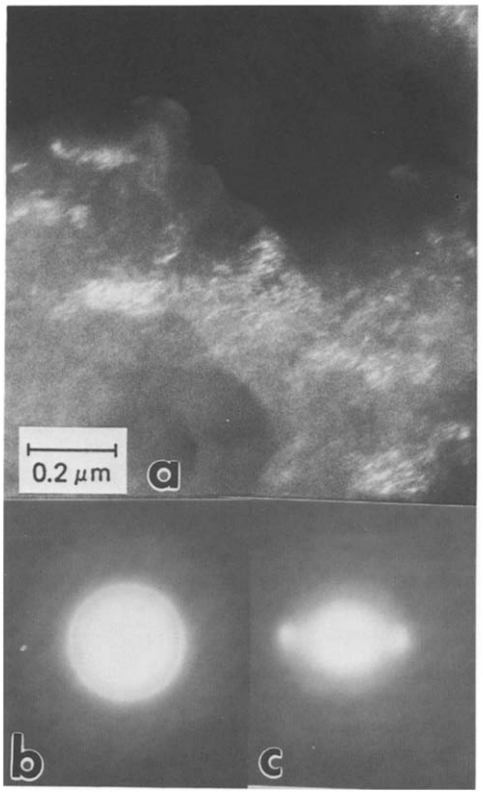

Figure 7 T.e.m. of 30% PBT/70% ABPBI vacuum cast copolymer film showing (a) dark field image, (b) s.a.e.d. pattern from 5 μm area, and (c) s.a.e.d. pattern from 0.1 μm area

one of the characteristic ABPBI equatorial reflections increase in value when considering first the sample of pure PBT or pure ABPBI, then the physical blend $C < C_{cr}$ spun fibre, and finally the copolymer $C < C_{cr}$ spun fibre. The characteristic ABPBI spacing increases from 0.716 to 0.737 to 0.797 nm as the samples progress from pure ABPBI, to ABPBI in physical blend fibre, to ABPBI in copolymer fibre. This indicates that the edges of the planes of the heterocyclic rings in the unit cell are being pushed further apart laterally. In the physical blend fibre it is likely that the increase in the spacing is due to some mixing of PBT molecules in the ABPBI crystal which perturbs the lattice. In the copolymer fibre the spacing of the planar edges of the heterocyclic rings is even larger and there is evidently more mixing of PBT molecules in the ABPBI crystallites and greater perturbation of the lattice.

A similar trend is observed for the characteristic PBT spacing which increases from 0.579 to 0.611 to 0.634 nm as the samples progress from pure PBT, to PBT in the physical blend fibre, to PBT in the copolymer fibre. It appears that ABPBI is probably mixing in the crystallites of PBT, thus perturbing the lattice and increasing spacing of the planar edges of the hererocyclic rings. Only a very small increase in spacings occurs for the 0.35 nm reflection which is the planar spacing between the planes of the heterocyclic rings in both PBT and ABPBI crystallites. This indicates that any mixing of the ABPBI in PBT crystallites occurs chiefly at the edges of the planes of the heterocyclic rings rather than between the planes of the heterocyclic rings. The same conclusion would also hold true for PBT mixing with ABPBI crystallites. Overall, the larger increase in d-spacing of both PBT and ABPBI at the edges of the planes of the heterocyclic rings of the block copolymer compared to the physical blend indicates that molecules are mixing more intimately in the copolymer than in the polymer blend.

Transmission electron microscopy (t.e.m.)

Cast copolymer film. Figure 7a is a dark field image of an ion-thinned section of the cast copolymer film. There are a few regions in white that are about 100 nm high and 100–200 nm wide. Each region is composed of much smaller white 'flakes' which are diffracting crystallites. These crystallites have sizes in the order of 10 nm.

A typical s.a.e.d. pattern for a larger 5 μm diameter area of electron beam illumination is shown in *Figure 7b* in the lower left corner of the micrograph. This larger area s.a.e.d. pattern shows that there is no overall orientation of crystallites within the film. However, when an s.a.e.d. pattern is obtained from a 0.1 μm area within a particle, as shown in *Figure 7c* on the lower right side, it contains relatively sharp and moderately well-arced equatorial reflections with spacing ratios characteristic of PBT, indicating that there are large, moderately well-oriented PBT crystallites within the particles. Several orders of fairly sharp, but slightly curved, meridional reflections are present, indicating moderate molecular orientation. The meridional (0 0 1) spacing of PBT was used as a standard to calculate the d-spacings of the equatorial reflections. The presence of the 0.60 nm reflection confirms that crystallites are PBT. This agrees with the s.e.m. results which showed that the 0.1 μm particles seen here in dark field imaging are composed chiefly of PBT. Additionally, it has been found from the orientation of the diffraction pattern that the chain axis of the PBT molecules and *c*-axis of the crystallites are aligned perpendicular to the wider dimension of the platelets and particles.

From the above results, it is concluded that 30% PBT/70% ABPBI $C > C_{cr}$ copolymer film contains phase-separated particles within a ductile matrix. These particles are chiefly composed of a lateral agglomeration of moderately oriented 8–10 nm wide PBT crystallites. This supports the model for the morphology of the cast copolymer film shown in *Figure 4a*.

Spun copolymer fibre. The t.e.m. dark field image from the (h k 0) reflections of the fibre spun from 30% PBT/70% ABPBI $C < C_{cr}$ solution is shown in *Figure 8a*. There are no obviously discernable features greater than 3 nm in size. From this observation and limitations of the statistical resolution of the image, it can be concluded that the size of any crystallites that are present would have to be about 3 nm or less.

Figure 8b shows the s.a.e.d. pattern for $C < C_{cr}$ fibre. It contains a broad moderately well-arced equatorial reflection at 0.84 nm. This indicates that ABPBI crystallites are present, but that they are very small and/or disordered. This is in agreement with the dark field results. The 0.35 nm reflection is a composite reflection for PBT and ABPBI structures. It indicates that PBT and/or ABPBI crystallites may be present. The moderate arcing of the equatorial reflections indicates moderate crystallite orientation along the fibre axis. The above s.a.e.d. results are similar to WAXS results which also indicate the presence of small and/or disordered crystallites which are moderately oriented. The broad and somewhat curved meridional reflections indicate that there is also good orientation of the molecules with respect to the fibre axis. The presence of three meridional orders characteristic of ABPBI meridional reflections

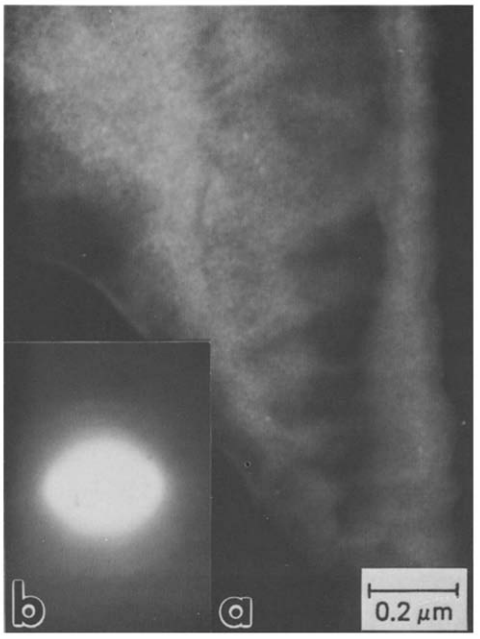

Figure 8 T.e.m. of 30% PBT/70% ABPBI spun copolymer fibre showing (a) dark field image and (b) s.a.e.d. pattern

indicates that the ABPBI molecules are well enough oriented and ordered to produce meridional reflections. Although the diffuseness of the pattern makes measurement of spacings difficult, there are clearly two distinct sets of meridional spacings present. Measurement of the spacings indicates that oriented molecules of both PBT and ABPBI are present.

It is concluded from the dark field images and s.a.e.d. patterns that 30% PBT/70% ABPBI $C < C_{cr}$ copolymer fibre contains small, moderately well oriented crystallites of PBT and ABPBI which are no larger than 3 nm in diameter. The t.e.m. images show that no crystalline phase separation occurs at a scale larger than 3 nm for either the fibre or the film. The PBT and ABPBI components have been dispersed at a scale finer than 3 nm. Thus, a molecular level composite has been formed in the copolymer fibre. A model for the morphology of the 'molecular composite' copolymer fibre is shown in *Figure 4b*.

General discussion

When copolymer film is vacuum cast from 30% PBT/70% ABPBI $C > C_{cr}$ solution, s.e.m. and t.e.m. images show that phase separation occurs and platelets and particles 0.1–0.4 μm are formed. T.e.m. reveals that these phase-separated particles are composed of crystallites which are about 8–10 nm size, and s.a.e.d. indicates the crystallite *c* axis and molecules are oriented perpendicular to the width of the platelet.

It can be concluded that the crystallites in the particles are chiefly PBT. First, s.a.e.d. patterns reveal crystallites of PBT present in the particles. It is unlikely that there are crystallites of ABPBI present within the particles. Flory's theory of rigid-rod phase equilibria[21,22] actually predicts total exclusion of the flexible molecules from the rod-rich phase, but it may, however, be possible that some ABPBI exists within the particles as a non-crystalline material.

The matrix is chiefly composed of ABPBI since there is less PBT than ABPBI in the total sample (30% PBT/70% ABPBI) and relatively little PBT would be left in the matrix material if the particles are mostly PBT. The matrix of the phase-separated film showed some ductility in s.e.m. micrographs similar to the ductility observed in s.e.m. photos of fractured ABPBI fibres. This is probably due both to the lack of orientation and the reduced amount of PBT in the matrix. Thus, these data indicate the matrix is chiefly ABPBI. This is in agreement with Flory's theory which predicts some, but little, rigid-rod polymer will still be present in the coil phase.

The modulus and strength of the microphase-separated material are also relatively low because of the low aspect ratio of the PBT-rich particles which results in inefficient reinforcement of the matrix material. However, the mechanical properties are higher than those for the vacuum cast film of the physical blend. This is probably due to the smaller particles from reduced scale of the phase separation and improved adhesion between phases in the vacuum cast copolymer film.

When copolymer fibre is spun from 30% PBT/70% ABPBI $C < C_{cr}$ solution no large-scale phase separation is observed. The s.a.e.d. and WAXS patterns indicate that both PBT and ABPBI crystallites are present. T.e.m. dark field images reveal no features present at a scale larger than 3 nm demonstrating that a dispersion of PBT in ABPBI at a level of 3 nm or better has been achieved. Stated more conservatively, it can be said that no crystalline phase separation occurs at a scale larger than 3 nm. A copolymer coil/rod/coil with this level of dispersion is considered to be a molecular composite. Crystallites of PBT segments less than 3 nm in lateral size may be present in the molecular composite, but this cannot be determined from t.e.m. Thus, the aspect ratio of the reinforcing phase of PBT molecular segments and molecular segment bundles is very high in the molecular composite fibre compared with the PBT in particles in the phase-separated film. This results in more efficient reinforcement of the matrix. In the copolymer molecular composite fibre, s.a.e.d. patterns show that the PBT and ABPBI molecules and crystallites are also moderately well oriented. Both efficient reinforcement and orientation of ABPBI and PBT result in high values of mechanical properties in the copolymer molecular composite fibre. The values of its modulus and strength are, respectively, 43 and 8 times greater than those of the phase-separated film.

The value of elongation to break for the copolymer molecular composite fibre (2.4%) is dramatically reduced, by a factor of about 20, compared with that for the microphase-separated copolymer film (43%). This occurs because most of the reinforcing PBT has phase separated out of the matrix material in the phase-separated film, thus giving the matrix material a larger fraction of the more ductile ABPBI. Interestingly, the elongation to break is eight times higher for the cast copolymer film compared with the cast physical blend film. This is evidently due to the reduced scale of phase separation and the improved adhesion between the matrix and the particles in copolymer film.

There are some additional comparisons that can be made between the 'molecular composite' fibres of the copolymer and the physical blend with respect to the mechanical properties of the PBT homopolymer fibre. Since, in general, elongation to break decreases with increasing fibre orientation, it can be considered a crude

measure of orientation of crystallites and molecules within the fibre. The elongation to break in the physical blend fibre is 1.4% compared with 1.1% in the PBT fibre. This indicates that it might be possible to slightly improve the orientation in the physical blend fibre. However, in the copolymer fibre the elongation to break is 2.4%, more than double that for the PBT fibre. This indicates that it might be possible to moderately increase the orientation of the copolymer fibre and achieve corresponding increases in modulus and tensile strength. Also, since the s.e.m. micrograph of the copolymer fibre showed 30–40% voids in the fibre interior, the mechanical properties could actually be increased by more than 50% for a void-free fibre. Thus, it is not unreasonable to project that, with optimum processing conditions, the modulus and tensile strength of the copolymer fibre could be increased by a factor of 1.5–2.

A doubling of the modulus would, of course, significantly exceed the modulus predicted by the 'rule of mixtures' for uniaxially reinforced composites. However, the application of the 'rule of mixtures' has been assumed to be a simplified approach based on the measured values of properties of the component materials, not the theoretically predicted values. The theoretically predicted value of the modulus of PBT is 615 GPa, almost double the value of the highest *measured* modulus[25]. By applying the theoretical modulus to the 'rule of mixtures' for the 30% PBT/70% ABPBI copolymer fibre, it should be possible, with perfect orientation, to achieve a modulus of about 180 GPa, which is double the currently measured value and almost equal to the value of steel. This would yield a specific modulus about eight times that of steel. The potential for superior mechanical properties of copolymer molecular composites is excellent, but additional work is necessary for optimizing processing conditions and for improved modelling for property prediction.

ACKNOWLEDGEMENTS

We gratefully acknowledge partial support of this research from the Chevron Research Company and for partial support for the s.e.m. and accessories from the National Science Foundation Materials Instrumentation Research Fund.

REFERENCES

1 Helminiak, T. E., Benner, C. L., Arnold, F. E. and Husman, G. E. US Pat. Appl. 902 525, 1978
2 Husman, G., Helminiak, T., Adams, W., Wiff, D. and Benner, C. *Am. Chem. Soc. Symp. Ser.* 1980, **132**, 203
3 Takayanagi, M., Ogata, T., Morikawa, M. and Kai, T. *J. Macromol. Sci. Phys.* 1980, **B17**, 519
4 Takayanagi, M. *Pure Appl. Chem.* 1983, **55**, 819
5 Hwang, W.-F., Wiff, D. R., Benner, C. L. and Helminiak, T. E. *J. Macromol. Sci. Phys.* 1983, **B22**, 231
6 Krause, S. J. and Adams, W. W., Proceedings, 41st EMSA Meeting, San Francisco Press, San Francisco, 1983, p. 32
7 Krause, S. J., Haddock, T., Price, G. E., Lenhert, P. G., O'Brien, J. F., Helminiak, T. E. and Adams, W. W. *J. Polym. Sci., Polym. Phys. Edn.* 1986, **24**, 1991
8 Tsai, T. T., Arnold, F. E. and Hwang, W. F. *Am. Chem. Soc. Polym. Prepr.* 1985, **26**, 144
9 Adams, W. W., Azaroff, L. V. and Kulthreshthra, A. K. *Z. Kristal.* 1980, **150**, 321
10 Roche, E. J., Takahashi, T. and Thomas, E. L. *Am. Chem. Soc. Symp. Ser.* 1980, **141**, 303
11 Odell, J. A., Keller, A., Atkins, E. D. T. and Miles, M. J. *J. Mater. Sci.* 1981, **16**, 3309
12 Minter, J. R., Shimamura, K. and Thomas, E. L. *J. Mater. Sci.* 1981, **16**, 3303
13 Shimamura, K., Minter, J. R. and Thomas, E. L. *J. Mater. Sci. Lett.* 1983, **2**, 54
14 Allen, S. R., Farris, R. J. and Thomas, E. L. *J. Mater. Sci.* 1985, **20**, 4583
15 Allen, S. R., Farris, R. J. and Thomas, E. L. *J. Mater. Sci.* 1985, **20**, 2727
16 Feldman, L., Farris, R. J. and Thomas, E. L. *J. Mater. Sci.* 1985, **20**, 2719
17 Helminiak, T. E. *Am. Chem. Soc. Org. Coat. Plast. Chem.* 1979, **40**, 475
18 Fratini, A. V., Cross, E. M., O'Brien, J. and Adams, W. W. *J. Macromol. Sci. Phys.* 1985–1986, **B24**, 159
19 Christensen, R. M. in 'Mechanics of Composite Materials', Wiley, New York, 1979, pp. 89–99
20 Hwang, W.-F., Wiff, D. R., Verschoore, C., Price, G. E., Helminiak, T. E. and Adams, W. W. *Polym. Eng. Sci.* 1982, **23**, 784
21 Flory, P. J. Proc. R. Soc. London 1956, **A234**, 73
22 Flory, P. J. *Macromolecules* 1978, **11**, 1138
23 Northolt, M. G. and van Aartsen, J. J. *J. Polym. Sci., Polym. Symp.* 1977, **58**, 283
24 Li, L. S., Allard, L. F. and Bigelow, W. C. *J. Macromol. Sci. Phys.* 1983, **B22**, 269
25 Stewart, J., personal communication